

Electrochemical reduction process of Co(II) in citrate solution

Yan LIU¹, Zhe-jun LI¹, Yi-cheng WANG², Wei WANG¹

1. School of Chemical Engineering, Tianjin University, Tianjin 300072, China;
2. Faculty of Metallurgy and Energy Engineering, Kunming University of Science and Technology, Kunming 650093, China

Received 27 March 2013; accepted 7 September 2013

Abstract: Effects of citrate concentration and pH on the electrochemical reduction process of Co(II) were investigated by cyclic voltammetry(CV) and electrochemical impedance spectroscopy(EIS). The results show that Co(II) is reduced into two species which are free Co^{2+} and $[\text{Co}(\text{C}_6\text{H}_6\text{O}_7)]$ in the solution composed of 0.05 mol/L $\text{CoSO}_4 \cdot 5\text{H}_2\text{O}$, 0.20 mol/L Na_2SO_4 and 0–0.40 mol/L $\text{C}_6\text{H}_5\text{O}_7\text{Na}_3 \cdot 2\text{H}_2\text{O}$ in the pH range of 3–9. The reduction behavior depends on the pH of the solution. Co(II) is mainly reduced into the form of free Co^{2+} at pH 3 and into the form of $[\text{Co}(\text{C}_6\text{H}_6\text{O}_7)]$ at the pH range of 4–6 in citrate solution. The $[\text{Co}(\text{C}_6\text{H}_6\text{O}_7)]$ is first reduced to an intermediate state and then to Co^0 . Adsorption of the intermediate state exists on the surface of the electrode. Co(II) is difficult to be reduced in the solution with the pH above 7, because the existing Co(II)-citrate complex species $[\text{Co}(\text{C}_6\text{H}_5\text{O}_7)]^-$ and $[\text{Co}(\text{C}_6\text{H}_4\text{O}_7)]^{2-}$ are more difficult to be reduced than the hydrogen ion.

Key words: Co(II) ion; electrochemical reduction process; citrate; complex species

1 Introduction

Cobalt electrodeposits are usually used as functional coatings because of their high temperature resistance and anti-oxidation properties, and cobalt alloy electrodeposits [1–3] and multiplayer cobalt electrodeposits [4,5] have also attracted a great interest due to their advanced magnetic properties. Electrochemical reduction mechanism of Co(II) in citrate solution can provide theoretical guidance for the electro-deposition of cobalt and cobalt alloy. Some investigations have been devoted to the technologies and kinetics of cobalt electro-deposition in chloride solutions [6,7] or sulfate solutions [8–12]. The existing theoretical researches have been focused on the simple cobalt solution without any complexant or with ammonia only [10,13]. The nucleation mechanism [10–12] and underpotential [12,14] deposition have been of special concern.

It is necessary to add complexant such as citrate into the solutions to change the structure of the coatings and improve its performance during cobalt deposition. Some studies considering the influence of citrate during the cobalt electro-deposition have been reported. REHIM et

al [15] discussed effects of bath composition, current density, pH and temperature on the electro-deposition of cobalt by potentiodynamic cathodic polarization curves, and an optimum bath composition with 0.36 mol/L $\text{CoSO}_4 \cdot 7\text{H}_2\text{O}$, 0.19 mol/L citrate and 0.10 mol/L citric acid at pH 5.0 has been established. Some other investigations [16,17] on the morphology and structure of the cobalt coating obtained by electro-deposition in citrate solution were performed. However, more attentions have been paid to the exploitation of the deposition technology and characterization of the deposit, and seldom theoretical work has been performed on the electrochemical behavior and reduction mechanism of the cobalt deposition in citrate solutions, and also the electrochemical impedance spectroscopy analysis has been seldom applied.

Thus, the present work investigated systematically the effects of citrate concentration and pH on the electrochemical reduction process of Co(II) in citrate solution by CV and EIS. Especially, the complex species of Co(II) and citrate in the solution and their corresponding electrochemical reduction process were discussed, which was very important earlier stage work for exploiting the technology of cobalt alloy deposition.

2 Experimental

2.1 Solution preparation

All of the solutions were prepared with analytical reagents and redistilled water to ensure the stability of ions in the solution. The solution compositions are listed in Table 1. A pHS-2C precision acidity meter was used to measure the pH value of the solutions. And the pH value was adjusted by adding sodium hydroxide solution or sulfuric acid solution with the concentration of 20% (volume fraction).

Table 1 Composition of solutions

Solution No.	Composition/(mol·L ⁻¹)			pH value
	CoSO ₄ ·7H ₂ O	C ₆ H ₅ O ₇ Na ₃ ·2H ₂ O	Na ₂ SO ₄	
1	0.05	—	0.20	5.14
2	0.05	0.05	0.20	5.50
3 ^[a]	0.05	0.10	0.20	5.72
4	0.05	0.15	0.20	6.06
5	0.05	0.20	0.20	6.42
6	0.05	0.40	0.20	6.90

^[a] The pH of solution 3 was adjusted to different values for investigating the effect of pH value.

2.2 Electrochemical measurement

The electrochemical measurements were carried out by a PARSTAT 2273 (Princeton Applied Research) at (25±1) °C. A conventional three-electrode cell was adopted. The working electrode was a pure Au plate with a working area of 1.0 cm×1.0 cm. The auxiliary electrode was a platinum plate with a working area of 3.5 cm×6.5 cm. And the reference electrode was a saturated calomel electrode (SCE). The working electrode was polished with a cloth-wheel, and then degreased by cathodic electrolysis in alkaline solution to ensure a smooth and clean surface before measurement. The solutions were not stirred during the measurement.

The cyclic voltammogram measurement was started at the opening circuit potential with the scanning rate of 200 mV/s, and the first cycle was recorded. All the potentials in this work referred to the SCE reference electrode, and the cathodic current was set as being positive. The EIS measurements were performed in the frequency range of 10 mHz to 100 kHz with signal amplitude of ±5 mV.

3 Results

3.1 Effects of citrate concentration on electrochemical reduction process of Co(II)

The CV curves of Au electrode in solutions with various citrate concentrations (Solutions No. 1–6 in Table 1)

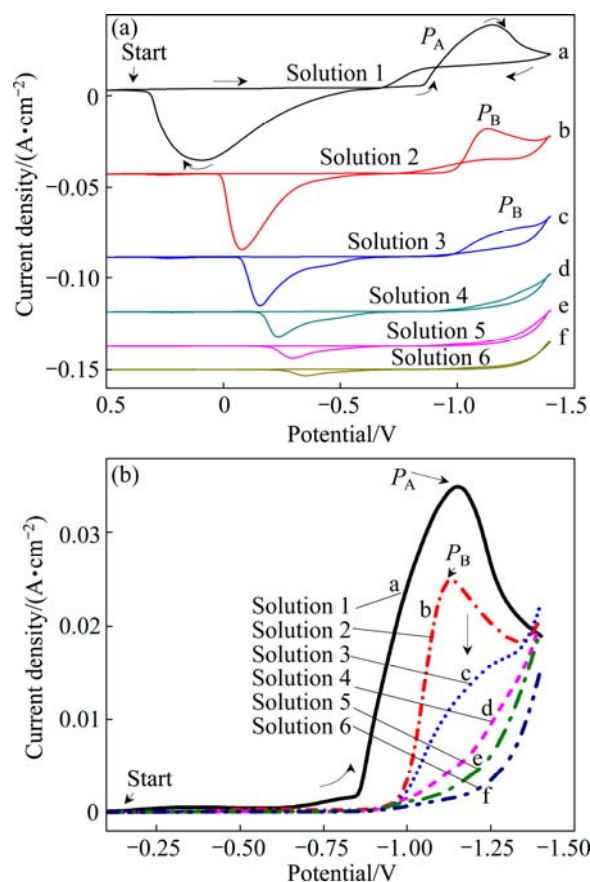


Fig. 1 CV curves of Au electrode in solutions with various citrate concentrations: (a) Whole curves; (b) Amplified curves of cathodic-scanning peaks

are shown in Fig. 1. The scanning potential range is from 0.5 to -1.4 V. Figure 1(a) shows the whole CV curves, and Fig. 1(b) illustrates the amplified CV curves of the cathodic scanning peaks. Only one sharp reduction peak (peak P_A) with the initial potential of -0.8 V is observed in the cathodic-going process of curve a. It is attributed to the reduction of free Co^{2+} to Co^0 . The initial potential of reduction peak P_B at curves b–f is about -1.0 V, and the peak current decreases gradually from curve b to curve f as the concentration of citrate increases. Hydrogen evolution starts at the potential of about -1.3 V in curve a and at about -1.4 V in curves b–f, respectively. It can be concluded that reduction of Co(II) becomes more difficult due to the formation of Co(II)-citrate complex when citrate is added. The peak current of P_B decreases with the increase of citrate concentration because concentration of the corresponding Co(II)-citrate complex is reduced. The Co(II)-citrate complex can turn to a kind of new and more stable Co(II)-citrate complex with the improving of citrate concentration, and the reduction potential of the complex is more negative than that of the hydrogen ion.

The CV curves of Au electrode in solution 2 were measured under different scanning rates, as shown in

Fig. 2(a), to get more information about peak P_B . The relationship between J_p and ν as well as J_p and $\nu^{1/2}$ for peak P_B , and their corresponding linear fitting results are shown in Fig. 2(b). According to the Langmuir isothermal adsorption rule, there is a linear relationship between J_p and ν if ion adsorption exists in the corresponding reactions, while J_p will change linearly with the extracting roots of scanning rate $\nu^{1/2}$ if the current peak is caused only by ion diffusion. It can be seen from Fig. 2(b) that there is a good linear relationship between J_p and ν for peak P_B , indicating that adsorption exists in the reduction process.

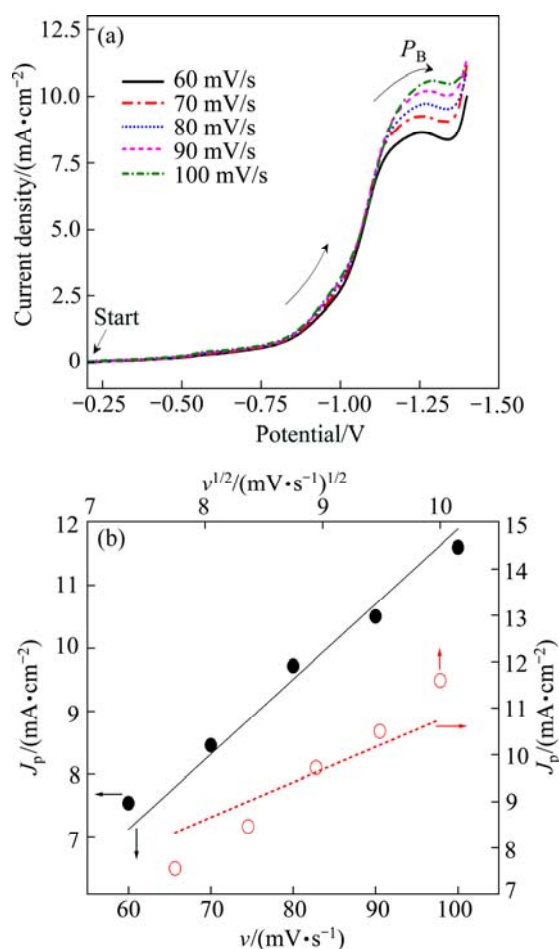


Fig. 2 CV images of Au electrode in solution 2 at different scanning rates: 60, 70, 80, 90, and 100 mV/s, respectively (a) and relationships between J_p and ν as well as J_p and $\nu^{1/2}$ for peak B in (b)

3.2 Effects of pH value on electrochemical reduction process of Co(II)

The CV curves of Au electrode in solution 3 at different pH values are shown in Fig. 3. The scanning potential range is from 0.5 to -1.4 V. Figure 3(a) shows the whole CV curves, and Fig. 3(b) illustrates the amplified CV curves of the cathodic scanning peaks. Results show that reduction process changes greatly with the variation of pH of the solution. Peak P_A starts at

about -0.8 V and peak P_C starts at about -1.0 V when the solution pH value is 3. With the increasing of the solution pH, current density of peak P_C gets weaker at pH 4 (curve b) and then disappears at pH 5 (curve c), peak P_B becomes weaker from pH 4 to 7 (curves b to e). When the pH of the solution is above 7 (curves f and g), no reduction peak is observed except the current of hydrogen evolution starts at about -1.4 V. The corresponding oxidation peaks in the CV curves at pH 8 and 9 is almost not seen either. The current efficiency of cobalt deposition in the solution is 70.5% at pH 5 and 12.1% at pH 8, respectively, at the current density of 10 mA/cm². Both the CV results and the current efficiency results lead to the same conclusion that cobalt is very difficult to be deposited from basic citrate solution in the pH range of 8–9.

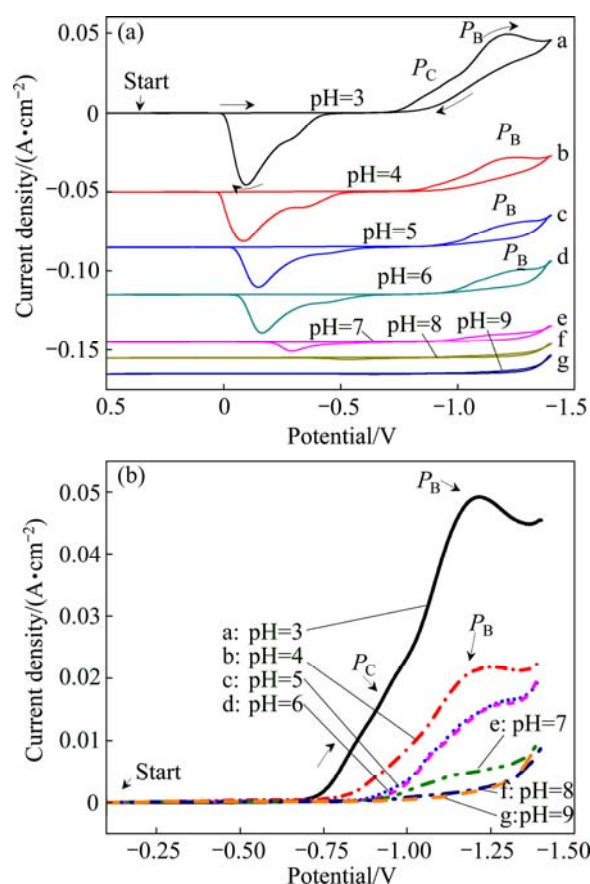


Fig. 3 CV curves of Au electrode in solutions composed of 0.05 mol/L $\text{CoSO}_4 \cdot 7\text{H}_2\text{O}$, 0.20 mol/L Na_2SO_4 and 0.10 mol/L $\text{C}_6\text{H}_5\text{O}_7\text{Na}_3 \cdot 2\text{H}_2\text{O}$ (solution 3) at different pH value: (a) Whole curves; (b) Amplified curves of cathodic-scanning peaks

3.3 EIS analyses

The electrochemical reduction kinetics of the three reduction peaks (P_A , P_B and P_C) are investigated by EIS. The measuring potentials are shown in Fig. 4, and the EIS results are shown in Fig. 5.

Figures 5(a) and (a') show the Nyquist and Bode plots measured at the potentials of -0.75 and -0.85 V

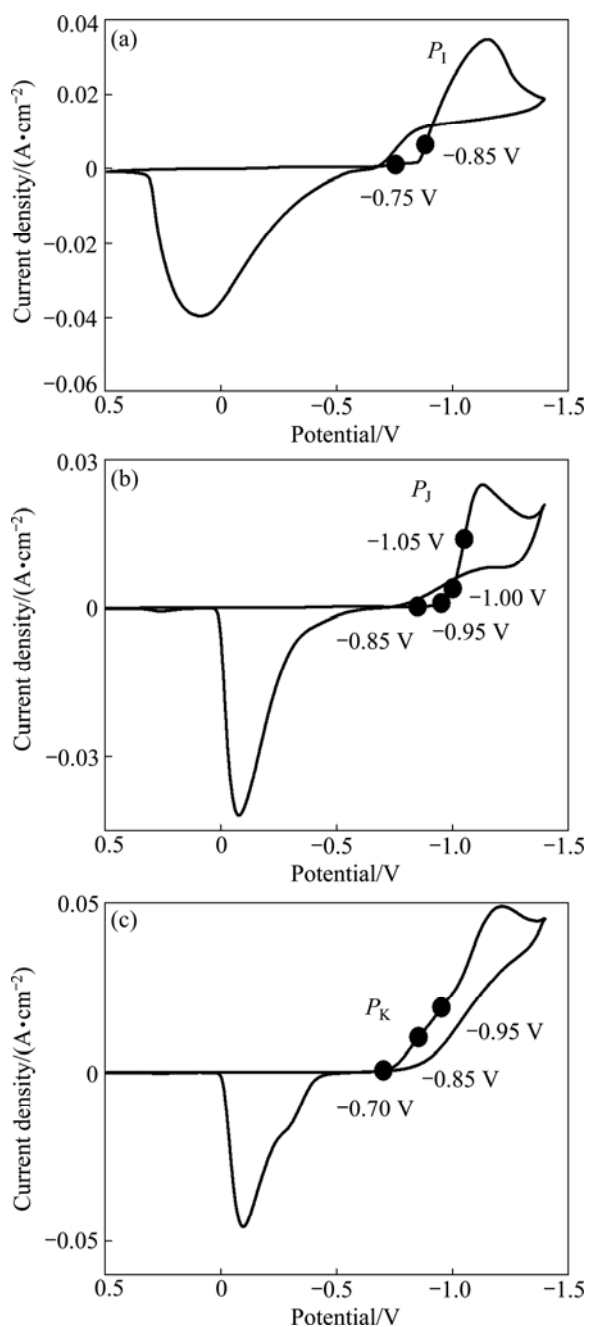


Fig. 4 Corresponding potentials in CV curves used for EIS measurement: (a) Curve a in Fig. 1, peak P_A ; (b) Curve b in Fig. 1, peak P_B ; (c) Curve a in Fig. 3, peak P_C

(the potential range of peak P_A in Fig. 4). It can be seen that the Nyquist plots measured at -0.75 V are composed of a large capacitive loop, indicating that one electrochemical reaction takes place, and the resistance of the reaction is large at this potential. As the potential shifts to -0.85 V, the Nyquist plots comprise a small capacitive loop in the high frequency range followed by a straight line in the low frequency (as shown in the inset of Fig. 5(a)), and the Bode plots contain two peaks. The peak in the low frequency of the Bode plots is caused by the finite diffusion of the reactant [18]. It reveals that the

electrochemical reaction carries out easily and diffusion of the reactant is the controlling step. Considering the above CV analyses, it can be concluded that diffusion of Co^{2+} to the surface of the electrode is the controlling step during the reduction of Co^{2+} to Co^0 .

The Nyquist and Bode plots measured at the potentials of -0.85 , -0.95 , -1.00 and -1.05 V (the potential range of peak P_B in Fig. 4) are shown in Figs. 5(b) and (b'). The Nyquist plots measured at -0.85 V comprise two sections: a capacitive loop in the high frequency range and an inductive loop in the low frequency range. The existence of the inductive loop located in the fourth quadrant is arisen by the adsorption–desorption behavior, which coincides well with the CV result. As the potential becomes more negative, the Nyquist plots turn to a capacitive loop in the high frequency range and an inductive loop followed by another capacitive loop in the low frequency range, respectively. The Bode plots contain two peaks, indicating that the reduction process contains two reactions. Combining the CV results, it is known that peak P_B is caused by the reduction of the Co(II) -citrate complex. It is concluded that the reduction is accomplished by two steps, and the existence of the inductive loop located in the fourth quadrant could be aroused by the adsorption and desorption of intermediate product. Thus, several possible equivalent circuits were proposed according to the above analyses of the Nyquist and Bode plots, and the best-fit circuit is shown in Fig. 6. The EIS results of peak P_B at -0.85 , -0.95 , -1.00 and -1.05 V were fitted in the frequency range of 10 mHz to 10 kHz according to the equivalent circuit (Fig. 6). The fitting results are shown in Fig. 7. In the equivalent circuit, R_s is the bulk solution resistance; C_1 is the double layer capacitance; R_1 is the resistance of the reduction of Co(II) -citrate to the intermediate state; L is the equivalent inductance caused by the adsorption and desorption; R_L is the equivalent resistance; C_2 is the capacitance of the reduction of the intermediate state to Co^0 ; R_2 is the resistance of the reduction of the intermediate state to Co^0 . It is concluded that the Co(II) -citrate is first reduced to an intermediate state and then to Co^0 , adsorption and desorption of the intermediate state exist on the surface of the electrode. The values of the electrochemical parameters of the best-fit equivalent circuits at -0.95 , -1.00 and -1.05 V are listed in Table 2. It could be found that all the electrochemical parameters change regularly as the potential decreases. The resistance of the reduction of Co(II) -citrate to the intermediate state decreases with the decrease of the potential, while that of the intermediate state to Co^0 increases with the decrease of the potential. The equivalent inductance caused by the adsorption and desorption becomes weaker at more negative potential.

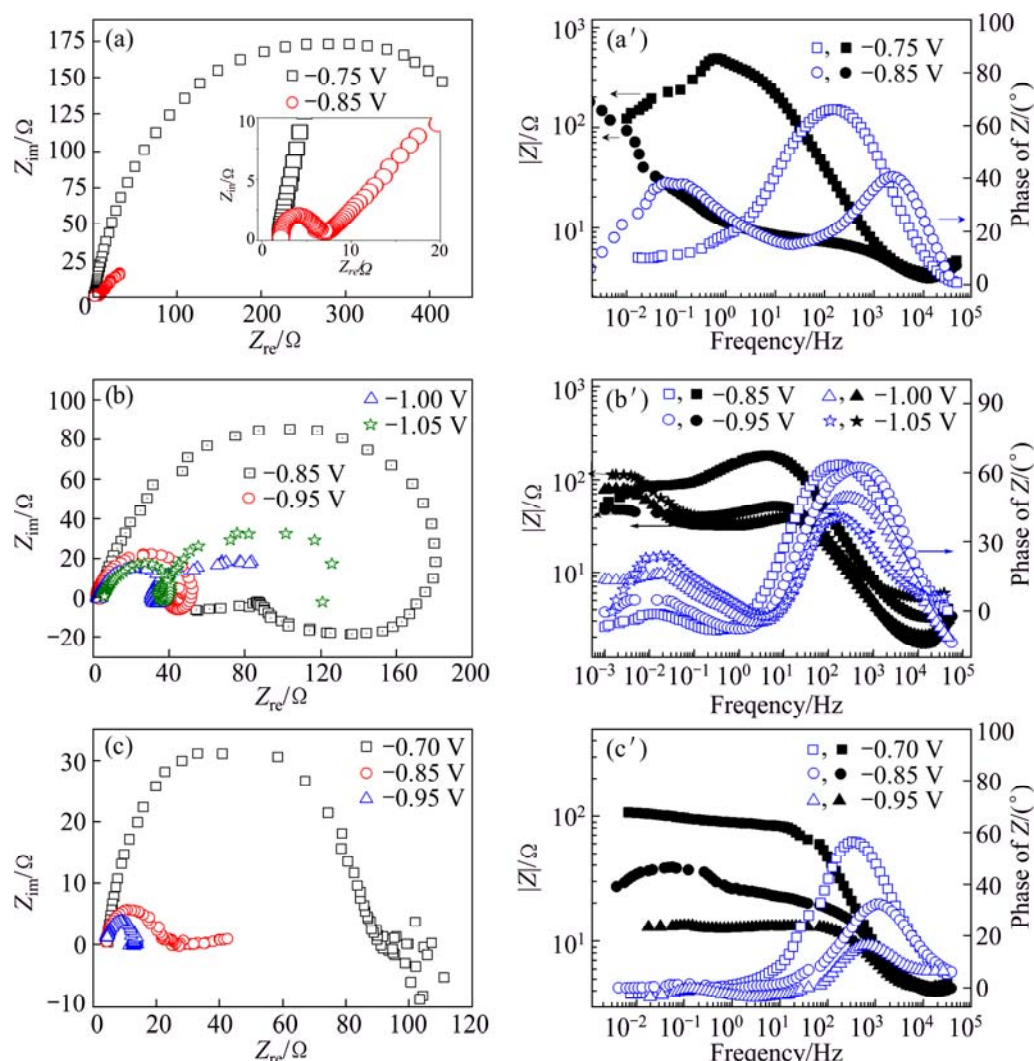


Fig. 5 EIS plots measured at different potentials of peak P_A , P_B and P_C in different solutions: (a) Nyquist plots of peak P_A in solution 1; (a') Bode plots of peak P_A in solution 1; (b) Nyquist plots of peak P_B in solution 2; (b') Bode plots of peak P_B in solution 2; (c) Nyquist plots of peak P_C in solution 3; (c') Bode plots of peak P_C in solution 3

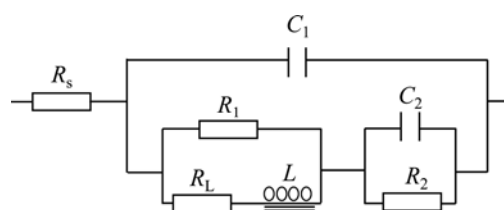


Fig. 6 Equivalent circuit for Co(II)-citrate complex reduction at potentials of -0.85 , -0.95 , -1.00 and -1.05 V in solution composed of 0.05 mol/L $\text{CoSO}_4 \cdot 5\text{H}_2\text{O}$, 0.20 mol/L Na_2SO_4 and 0.05 mol/L $\text{C}_6\text{H}_5\text{O}_7\text{Na}_3 \cdot 2\text{H}_2\text{O}$

Figures 5(c) and (c') show the Nyquist and Bode plots measured at the potentials of -0.75 , -0.85 and -0.95 V (the potential range of peak P_C in Fig. 4). The Nyquist plots are composed of a capacitive loop, and the radius of the capacitive loop reduces as the potential shifts negatively. The Bode plots possess only one peak, and the reduction resistance becomes smaller as the potential turns negative.

4 Discussion

The results of CV show that three cathodic reduction peaks (P_A , P_B and P_C) appear in the Co(II)-citrate solution within the pH range of 3–9. Those different reduction peaks attribute to the various Co(II) species existing in the solution and to be reduced on the surface of the electrode. Different Co(II)-citrate complex species are formed in the citrate solution, the distribution curve [19] obtained in the solution with the most similar composition in our research is cited, as shown in Fig. 8.

The existing Co(II)-citrate complex species are $[\text{Co}(\text{C}_6\text{H}_5\text{O}_7)]^-$ and $[\text{Co}(\text{C}_6\text{H}_4\text{O}_7)]^{2-}$ at pH 8–9 according to Fig 8. Considering that the current efficiency of cobalt reduction is very low in citrate solution at pH 8–9, it can be concluded that reduction potentials of $[\text{Co}(\text{C}_6\text{H}_5\text{O}_7)]^-$ and $[\text{Co}(\text{C}_6\text{H}_4\text{O}_7)]^{2-}$ are more negative than the hydrogen

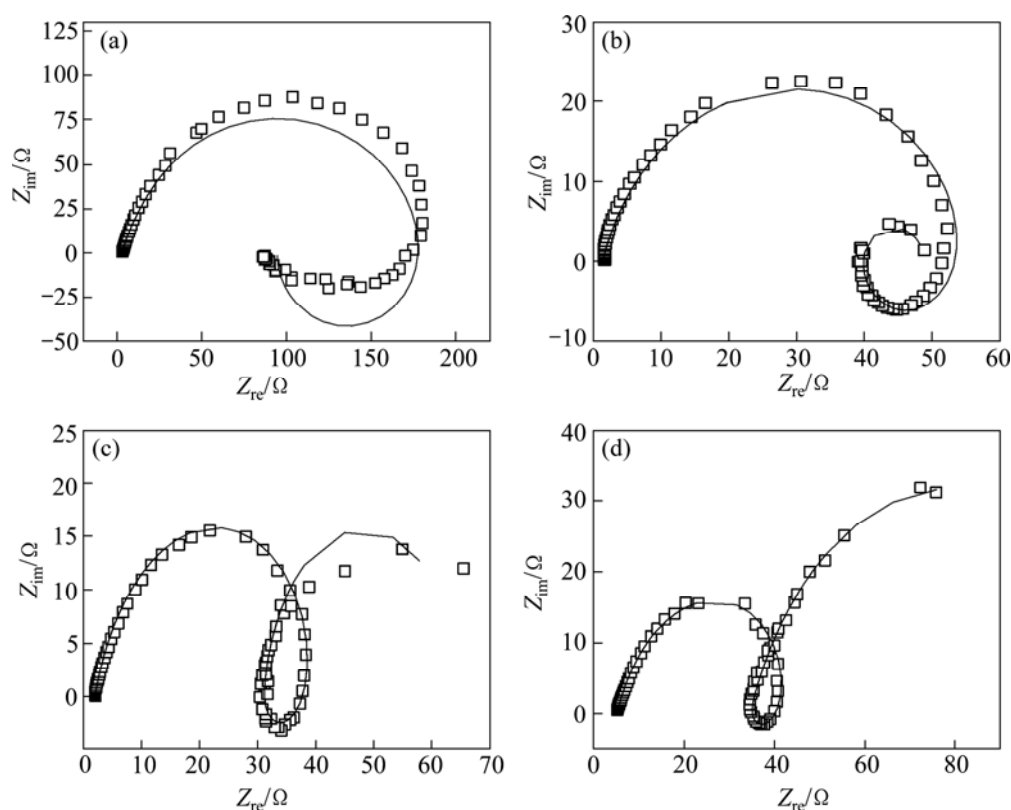


Fig. 7 Fitting curves of Nyquist plots measured at potentials of -0.85 V (a), -0.95 V (b), -1.00 V (c) and -1.05 V (d) in solution composed of 0.05 mol/L $\text{CoSO}_4 \cdot 5\text{H}_2\text{O}$, 0.20 mol/L Na_2SO_4 and 0.05 mol/L $\text{C}_6\text{H}_5\text{O}_7\text{Na}_3 \cdot 2\text{H}_2\text{O}$

Table 2 Fitted values of electrochemical parameters of equivalent circuits at -0.95 , -1.00 and -1.05 V in solution composed of 0.05 mol/L $\text{CoSO}_4 \cdot 5\text{H}_2\text{O}$, 0.20 mol/L Na_2SO_4 and 0.05 mol/L $\text{C}_6\text{H}_5\text{O}_7\text{Na}_3 \cdot 2\text{H}_2\text{O}$

Potential/V	$R_s/(\Omega \cdot \text{cm}^2)$	$Q_1/(\text{F} \cdot \text{cm}^2)$	$R_1/(\Omega \cdot \text{cm}^2)$	$L/(\text{H} \cdot \text{cm}^2)$	$R_2/(\Omega \cdot \text{cm}^2)$	$Q_2/(\text{F} \cdot \text{cm}^2)$	$R_3/(\Omega \cdot \text{cm}^2)$
-0.95	1.4	1.7×10^{-4} (n 0.83)	56.9	13.2	118.7	2.5 (n 0.97)	9.0
-1.00	2.0	2.4×10^{-4} (n 0.81)	53.6	2.9	88.4	0.3 (n 0.94)	34.3
-1.05	2.1	2.8×10^{-4} (n 0.78)	47.4	1.7	79.2	0.1 (n 0.78)	90.3

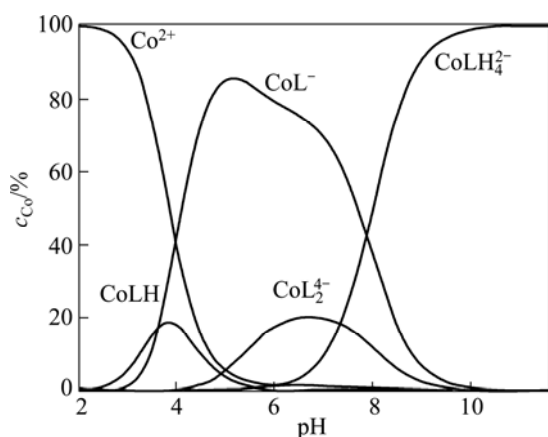


Fig. 8 Speciation curves for complexes formed in Co(II)-citrate system at 1:2 molar ratio of metal ions to ligand investigated by KOTSAKIS et al [19] (L refers to cit^{3-} with molecular formula of $\text{C}_6\text{H}_5\text{O}_7^{3-}$)

evolution potential. $[\text{Co}(\text{C}_6\text{H}_5\text{O}_7)]^-$ and $[\text{Co}(\text{C}_6\text{H}_5\text{O}_7)_2]^{4-}$ are the main existing species in the Co(II)-citrate solution when the pH of the solution is about 6. Higher coordinate complex is more stable than lower coordinate complex, thus, it is inferred that $[\text{Co}(\text{C}_6\text{H}_5\text{O}_7)_2]^{4-}$ is more stable than $[\text{Co}(\text{C}_6\text{H}_5\text{O}_7)]^-$, and also more difficult to be reduced on the surface of the electrode. Therefore, the reduction potential of $[\text{Co}(\text{C}_6\text{H}_5\text{O}_7)_2]^{4-}$ is also more negative than the hydrogen evolution potential. Co(II) exists as free Co^{2+} , $[\text{Co}(\text{C}_6\text{H}_5\text{O}_7)]^-$ and $[\text{Co}(\text{C}_6\text{H}_6\text{O}_7)]$ in weak acid citrate solution (pH 4–5), thus, peak P_B is ascribed to the reduction of $[\text{Co}(\text{C}_6\text{H}_6\text{O}_7)]$. Co(II) is reduced mainly into the form of $[\text{Co}(\text{C}_6\text{H}_6\text{O}_7)]$ in the citrate solution with the pH range of 4–5. Free Co^{2+} ion is the mainly species in the Co(II)-citrate solution at pH 3. There are two reduction peaks which are peak P_B and P_C in the CV curves at pH 3. The initial potential of peak P_C is close to that of the free Co^{2+} ion, leading to the

conclusion that peak P_C is also attributed to the reduction of free Co^{2+} to Co^0 . The CV results and the cited distribution curve coincide well.

Combining the CV and EIS results as well as the citing distribution curve, it can be concluded that peak P_A owns to reduction of free Co^{2+} directly to Co^0 by one step, while peak P_B refers to the reduction of $[\text{Co}(\text{C}_6\text{H}_6\text{O}_7)]$ which is first reduced to an intermediate state and then to Co^0 ; adsorption and desorption of the intermediate state exist on the surface of the electrode. Peak P_C is also attributed to the reduction of free Co^{2+} to Co^0 . The corresponding reduction reactions are listed in Table 3.

Table 3 Reactions of peak P_A , P_B and P_C

Peak	Reaction
P_A, P_C	$\text{Co}^{2+} + 2\text{e} \rightarrow \text{Co}^0$
P_B	$[\text{Co}(\text{C}_6\text{H}_6\text{O}_7)] + \text{e} \rightarrow \text{Inter}$,
	$\text{Inter} + \text{e} \rightarrow \text{Co}^0 + \text{C}_6\text{H}_6\text{O}_7^{2-}$

The cyclic voltammogram measurement was also performed on pure Cu substrate for comparison in cobalt solution (solution 1). It is found that the initial reduction potentials of free Co^{2+} to Co^0 are basically same on Cu substrate and Au substrate, which illustrates that the nucleation barriers of cobalt crystallization on Cu substrate and Au substrate are close. However, the adsorption behaviors of citrate may be very different on Cu substrate and Au substrate. Further investigations should be performed when the technology of cobalt deposition is exploited in citrate solution on Cu substrate in actual production.

5 Conclusions

1) Co(II) is reduced into two species which are free Co^{2+} and $[\text{Co}(\text{C}_6\text{H}_6\text{O}_7)]$ in the solution composed of 0.05 mol/L $\text{CoSO}_4 \cdot 5\text{H}_2\text{O}$, 0.20 mol/L Na_2SO_4 and 0–0.40 mol/L $\text{C}_6\text{H}_5\text{O}_7\text{Na}_3 \cdot 2\text{H}_2\text{O}$ in the pH range of 3–9.

2) The reduction potential shifts negatively obviously with the addition of citrate. The free Co^{2+} starts to be reduced at -0.8 V, while the reduction potential shifts to about -1.0 V with the addition of citrate due to the formation of $[\text{Co}(\text{C}_6\text{H}_6\text{O}_7)]$.

3) Variation of the solution pH value affects the reduction process greatly. Co(II) is mainly reduced into the form of free Co^{2+} at pH 3 in the citrate solution. $[\text{Co}(\text{C}_6\text{H}_6\text{O}_7)]$ is the mainly species reduced in weak acid citrate solution (pH range of 4–6). The EIS results show that the $[\text{Co}(\text{C}_6\text{H}_6\text{O}_7)]$ is first reduced to an intermediate state and then to Co^0 , and adsorption and desorption of the intermediate state exist at the surface of the electrode. When the pH value is above 7, cobalt is difficult to be

reduced at the surface of the electrode, because the existing Co(II)-citrate complex species, $[\text{Co}(\text{C}_6\text{H}_5\text{O}_7)]^-$ and $[\text{Co}(\text{C}_6\text{H}_4\text{O}_7)]^{2-}$, are more difficult to be reduced than the hydrogen ion.

References

- [1] GOMEZ E, PELLICER E, VALLES E. An approach to the first stages of cobalt–nickel–molybdenum electrodeposition in sulphate–citrate medium [J]. *Journal of the Electroanalytical Chemistry*, 2005, 580(2): 222–230.
- [2] DULAL S M S I, YUN H J, SHIN C B, KIM C K. Electrodeposition of CoWP film: III. Effect of pH and temperature [J]. *Electrochimica Acta*, 2007, 53(2): 934–943.
- [3] XU X, AZNGARI G. Electrodeposition of Co–P films from alkaline electrolytes [J]. *Journal of the Electrochemical Society*, 2007, 155(12): 742–749.
- [4] GOMEZ E, LALARTA A, LLORENTE A, VALLES E. Characterisation of cobalt/copper multilayers obtained by electrodeposition [J]. *Surface and Coatings Technology*, 2002, 153(2–3): 261–266.
- [5] PETER L, PADAR J, ROTH-KADAR E, CZIRAKI A, SOKI P, POGANY L, BAKONYI I. Electrodeposition of Co–Ni–Cu/Cu multilayers: 1. Composition, structure and magnetotransport properties [J]. *Electrochimica Acta*, 2007, 52(11): 3813–3821.
- [6] KONGSTEIN O E, HAARBERG G M, THONSTAD J. Current efficiency and kinetics of cobalt electrodeposition in acid chloride solutions. Part I: The influence of current density, pH and temperature [J]. *Journal of Applied Electrochemistry*, 2007, 37(6): 669–674.
- [7] CUI C Q, JIANG S P, TSEUNG A C C. Electrodeposition of cobalt from aqueous chloride solutions [J]. *Journal of the Electrochemical Society*, 1990, 137(11): 3418–3423.
- [8] RIOS-REYES C H, MENHOZA-HUIZAR L H, RIVERA M. Electrochemical kinetic study about cobalt electrodeposition onto GCE and HOPG substrates from sulfate sodium solutions [J]. *Journal of Solid State Electrochemistry*, 2010, 14(4): 659–668.
- [9] KABULSKA I F. Electrodeposition of cobalt on gold during voltammetric cycling [J]. *Journal of Applied Electrochemistry*, 2006, 36(2): 131–137.
- [10] GRUJUCIC D, PESIC B. Electrochemical and AFM study of cobalt nucleation mechanisms on glassy carbon from ammonium sulfate solutions [J]. *Electrochimica Acta*, 2004, 49(26): 4719–4732.
- [11] PALOMAR-PARDAVE M, SCHARIFKER B R, ARCE E M, ROMERO-ROMO M. Nucleation and diffusion-controlled growth of electroactive centers: Reduction of protons during cobalt electrodeposition [J]. *Electrochimica Acta*, 2005, 50(24): 4736–4745.
- [12] MENDOZA-HUIZAR L H, ROBLES J, PALOMAR-PARDAVE M. Nucleation and growth of cobalt onto different substrates, Part II. The upd-opd transition onto a gold electrode [J]. *Journal of the Electroanalytical Chemistry*, 2003, 545: 39–45.
- [13] RIOS R C. Kinetic study of the cobalt electrodeposition onto glassy carbon electrode from ammonium sulfate solutions [J]. *Quimica Nova*, 2009, 32(9): 2382–2386.
- [14] MENDOZA-HUIZAR L H, RIOS-REYES C H. Underpotential deposition of cobalt onto polycrystalline platinum [J]. *Journal of Solid State Electrochemistry*, 2011, 15(4): 737–745.
- [15] REHIM S S, WANAAB S M, IBRHIM M A M, DANKERIA M M. Electroplating of cobalt from aqueous citrate baths [J]. *Journal of Chemical Technology and Biotechnology*, 1998, 73(4): 369–376.
- [16] GOMEZ E, VALLES E. Thick cobalt coatings obtained by electrodeposition [J]. *Journal of Applied Electrochemistry*, 2002, 32(6): 693–700.

- [17] COHEN-HYAMS T, KAPLAN W D, YAHOLOM J. Structure of electrodeposited cobalt [J]. *Electrochemical and Solid-State Letters*, 2002, 5(8): C75–C78.
- [18] LI Fei-hui, WANG Wei, GAO Jian-ping, WANG Shuang-yuan. Electrochemical reduction process of Sb(III) on Au electrode investigated by CV and EIS [J]. *Journal of the Electrochemical Society*, 2009, 156(3): D84–D91.
- [19] KOTSAKIS N, RAPTOPOULOU C P, TANGOULIS V, TERZIS A, GIAPINTZAKIS J, JAKUSCH T, KISS T, SALIFOGLU A. Correlations of synthetic, spectroscopic, structural, and speciation studies in the biologically relevant cobalt(II)–citrate system: The tale of the first aqueous dinuclear cobalt(II)–citrate complex [J]. *Inorganic Chemistry*, 2003, 42(1): 22–31.

柠檬酸盐水溶液中二价钴的电化学还原过程

刘燕¹, 李喆珺¹, 王益成², 王为¹

1. 天津大学 化工学院, 天津 300072;

2. 昆明理工大学 冶金与能源工程学院, 昆明 650093

摘要: 采用循环伏安法(CV)和电化学交流阻抗法(EIS), 研究不同柠檬酸盐浓度和 pH 下钴的电化学还原过程。结果表明: 在组成为 0.05 mol/L $\text{CoSO}_4 \cdot 5\text{H}_2\text{O}$ 、0.20 mol/L Na_2SO_4 和 0~0.40 mol/L $\text{C}_6\text{H}_5\text{O}_7\text{Na}_3 \cdot 2\text{H}_2\text{O}$, pH 为 3~9 的溶液中, 二价钴以游离 Co^{2+} 离子和 $[\text{Co}(\text{C}_6\text{H}_5\text{O}_7)]$ 配合物两种形态存在, 并在电极表面被还原。溶液的 pH 对钴的电化学还原过程有显著的影响。当柠檬酸盐溶液的 pH 为 3 时, 钴主要以游离 Co^{2+} 离子的形态被还原; 当溶液为弱酸性(pH=4~6)时, 钴主要以 $[\text{Co}(\text{C}_6\text{H}_5\text{O}_7)]^-$ 的形态被还原为 Co^0 , 还原过程分两步进行, 中间产物在电极表面发生吸附; 当柠檬酸盐水溶液的 pH 大于 7 时, 形成的柠檬酸钴配合物主要是 $[\text{Co}(\text{C}_6\text{H}_5\text{O}_7)]^-$ 和 $[\text{Co}(\text{C}_6\text{H}_4\text{O}_7)]^{2-}$, 这两种配合物非常稳定, 其还原电位负于溶液的析氢电位, 因此难以从该溶液中还原得到 Co^0 。

关键词: 二价钴离子; 电化学还原过程; 柠檬酸盐; 络合物形态

(Edited by Chao WANG)